

Article

Studying the Thermoelastic Waves Induced by Pulsed Lasers Due to the Interaction between Electrons and Holes on Semiconductor Materials under the Hall Current Effect

Nidhal Becheikh ^{1,*}, Nejib Ghazouani ^{1,2}, Alaa A. El-Bary ^{3,4}  and Khaled Lotfy ^{5,6} ¹ College of Engineering, Northern Border University (NBU), Arar 73222, Saudi Arabia² Civil Engineering Laboratory, National Engineers School of Tunis (ENIT), University of Tunis El Manar, Tunis 1002, Tunisia³ Arab Academy for Science, Technology and Maritime Transport, Alexandria P.O. Box 1029, Egypt⁴ Council of Future Studies and Risk Management, Academy of Scientific Research and Technology, Cairo 4262104, Egypt⁵ Department of Mathematics, Faculty of Science, Zagazig University, Zagazig P.O. Box 44519, Egypt; khlotfy@zu.edu.eg⁶ Department of Mathematics, Faculty of Science, Taibah University, Madinah P.O. Box 344, Saudi Arabia

* Correspondence: nidhal.becheikh@nbu.edu.sa

Abstract: In the present work, the interaction between electrons and holes in semiconductor materials is investigated. According to the excitation process, the optical-elastic-thermal-diffusion (OETD) process is considered when the medium is exposed to a strong magnetic field and laser pulses. Photo-elastic and photo-electronics deformations are taken into account when the Hall current impact appears due to the magnetic field pressure on the semiconductor medium. Due to the complexity of the model, the governing equations that describe the system in one dimension (1D) are studied. Mathematical transformations (Laplace transform) were used to simplify the equations to obtain the physical quantities under study which were affected by laser pulses. To obtain complete solutions, some conditions were obtained from the free surface as well as from a mechanical ramp type and pulse heat flux, and then numerical transformations were applied using the inverse Laplace transform. Under the influence of several variables in this question, the results were explained graphically for silicon (Si) material and the results were analyzed in terms of their physical significance.

Keywords: holes and electrons; laser pulses; Hall current; silicon; photo-generated; semiconductors



Citation: Becheikh, N.; Ghazouani, N.; El-Bary, A.A.; Lotfy, K. Studying the Thermoelastic Waves Induced by Pulsed Lasers Due to the Interaction between Electrons and Holes on Semiconductor Materials under the Hall Current Effect. *Crystals* **2023**, *13*, 665. <https://doi.org/10.3390/cryst13040665>

Academic Editors: Mahmoud A.E. Abdelrahman and Emad El-Shewy

Received: 22 March 2023

Revised: 1 April 2023

Accepted: 7 April 2023

Published: 12 April 2023



Copyright: © 2023 by the authors. Licensee MDPI, Basel, Switzerland. This article is an open access article distributed under the terms and conditions of the Creative Commons Attribution (CC BY) license (<https://creativecommons.org/licenses/by/4.0/>).

1. Introduction

Through studying semiconductors, current physics research demonstrates that charge carriers in motion are particle-free but nevertheless transmit electric charges. Electrons, ions, and holes are only a few examples of the many distinct forms of charge carriers. In semiconductors, electrons and holes serve as the charge carriers. At zero Kelvin, free electrons populate the outermost atomic layers of semiconductors (the valence energy band). In these conditions, it is impossible for electrons or electric currents to move or switch positions. Increasing the temperature of a semiconductor causes its internal resistance to drop, which may allow some electrons to move from the valence band to the conduction band. To be more precise, an electric current is produced because electrons are moving about freely on the surface of the material. There will always be a vacancy in the valence band when an electron transitions to the conduction band. This causes electrons and holes in semiconductors to be physically near to one another. Electric currents flow through a semiconductor because of the motion of these free electrons. The holes also transfer electric currents in very unusual situations when the material is exposed to temperature gradients.

In recent years, scientists have been studying the Hall effect to learn more about the physics behind charge transport in semiconductors. When Edwin Hall [1] introduced a

magnetic field perpendicular to the direction of the current, he found that the locations and concentrations of electrons in semiconductor material deviated from a steady state. The electromotive force between the two particles is proportional to both the magnetic field and the current. The Hall effect occurs when electrons and holes move about due to the presence of a strong magnetic field. Hall voltage, current, and sample geometry may be monitored to determine the positive and negative conductivities of materials, notably semiconductors used in mobile chargers. Using a transistor and silicon oxide under the impact of a magnetic field as a semiconductor material, potential Hall measurements of a two-dimensional electron gas were made [2]. GaAs (Gallium arsenide) is a crossed-gap system, and it may hold both electrons and holes in equilibrium due to natural charge transfers [3]. A compensated quantum Hall plateau develops in perpendicular magnetic fields at the magnitude of the Hall resistance corresponding to the difference in occupancies of the electron and hole Landau levels, as shown by previous experimental investigations of this system with many more electrons than holes. This results right away in two interesting deviations from the standard single carrier model. To begin, the energy gap between Landau levels has no effect on the Hall resistance for a given sample [4]. The detection of several quantum Hall states is possible when the Hall resistance is identical but the number of occupied Landau levels varies. Second, the current distribution is substantially altered because the electron and hole edge states in the edge state picture are aligned along the same side of the sample. In a quantum Hall state of a two-dimensional (2D) electron system, the Fermi energy is positioned in a mobility gap between Landau levels when there is no net current flow between the bulk interior of the sample and the outside [5].

Both electronic (ED) and thermoelastic (TE) deformations occur in the study of semiconductors, particularly when a thermal (temperature) gradient is applied as a result of the absorbed optical light. As plasma waves are produced by the carrier density of holes and electrons, it follows that the ED is created when electrons and holes travel. The photothermal (PT) method might be utilized here. Nevertheless, thermal excitation processes cause a particle to vibrate, leading to the development of TE deformation. The photo-thermoelasticity (TE) hypothesis is created when ED and TE are taken into account together. Thermoelastic models were developed by Biot [6], Lord and Shulman [7], and Green and Lindsay (GL) [8] to take into consideration the impact of thermal and elastic relaxation durations on the governing equations of thermoelastic theory. This research provided support for the underlying scientific concepts by showing that waves may move at certain velocities. The generalized thermoelasticity (GTE) hypothesis has been applied to the study of elastic materials by a number of scientists [9–11]. The two-temperature theory is used inside the GTE framework to study the connections between thermal, elastic, and magnetic waves under the effect of gravity and thermal shock [12,13]. Maruszewski has investigated the relationship between the optical and elastic properties of a select group of semiconductor materials using a thermodynamic approach [14].

Several theoretical physical mathematical models for semiconductor materials [15,16] depict the overlap between thermal, elastic, and optical elastic features during diffusion transport processes of electron/hole charges. Semiconductors undergo an elastic-thermal-diffusive transport mechanism, the wave propagation of which was investigated by Sharma et al. [17]. Mass and heat diffusion may be measured by performing a photoacoustic sensitivity test on a semiconductor sample [18]. The photo-excitation of transport mechanisms in semiconductors may now be measured directly, thanks to technological advancements [19]. Several researchers subsequently linked the idea of thermoelasticity with the photothermal theory [20–24] to investigate the electronics, thermal, and elastic characteristics of semiconductor materials subjected to different external fields. Lotfy et al. looked at the Hall current impact of diffusive semiconductor material operating at microtemperatures and subjected to a magnetic field. A study by Mahdy et al. [25] examined how laser pulses exiting a semiconductor with fractional thermal order are affected by the electromagnetic field. The foregoing examination of photo-thermoelasticity

theory [26–31] does not account for the interaction between holes and electrons during thermo-diffusive processes.

This research looks at how a powerful magnetic field affects the Hall current as a consequence of electron-hole interactions. The effects of laser pulses on photo-generated charges in semiconductor media, including their optical, elastic, and thermal properties, are taken into account. The basic equation for electronics and thermoelastic deformation is reduced to one dimension (1D) when mass and heat are transmitted by thermo-diffusive processes. On the other hand, a unique mathematical model is developed to investigate photo-thermoelasticity cases of the semiconductor media subject to the influence of the Hall current. Analytical solutions of the principal fields are obtained by operating in the Laplace domain. To obtain the primary fields numerically, we approximate the Laplace transform inversion procedures. Numerical simulations of wave propagation for fundamental physical characteristics have been implemented in semiconductors using silicon's physical constants as an example. A graphical presentation and explanation of the findings are presented.

2. Basic Equations

An initially applied magnetic field $\vec{H} = (0, H_0, 0)$ along the y -axis is superimposed over a flawlessly conducting semiconductor material. In this case, the induced magnetic field $\vec{h} = h_i = (0, h_2, 0) = (0, h, 0)$ is generated along the same axis. Once optical energy plus a powerful magnetic field creates electronic/thermo-elastic deformation, an induced electric field $\vec{E} = E_i = (0, 0, E)$ perpendicular to \vec{h} is produced. The current density $J_r = (0, 0, J_3)$, on the other hand, is created in the same direction as \vec{E} . The semiconductor medium's linearized electromagnetic properties are satisfied in situations of isotropy and homogeneity with optoelectronics qualities (Figure 1) [32–37].

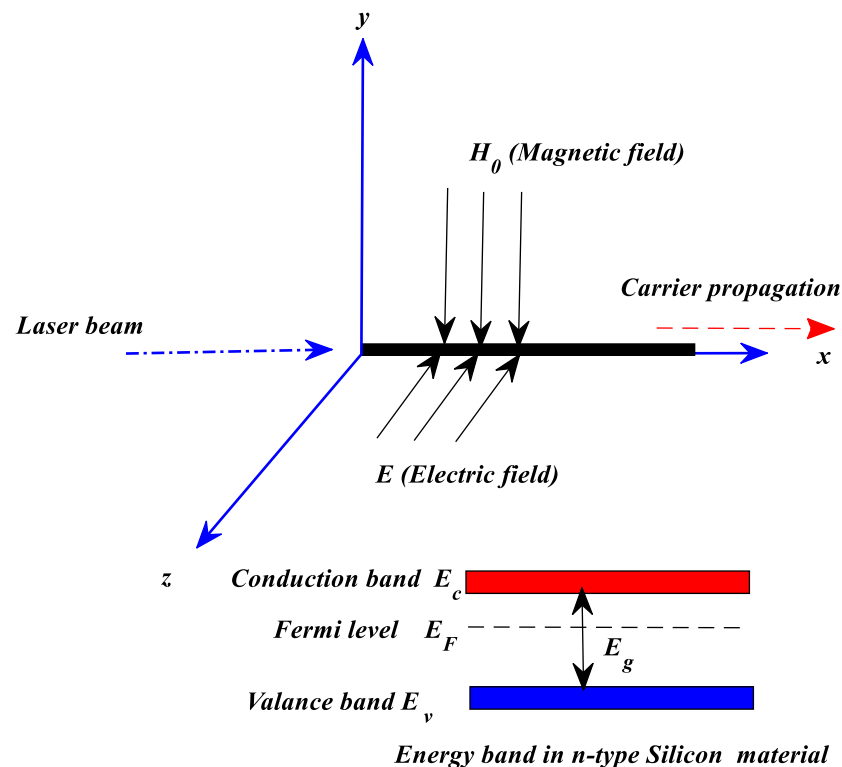


Figure 1. Schematic of the problem.

Ohm’s law for electromagnetic fields may be used to determine the Hall current, as shown below [38,39]:

$$\left. \begin{aligned} J_r &= \sigma_0 (E_i + \mu_0 \varepsilon_{ijr} (u_{j,t} - \frac{\mu_0}{en_e} J_j)) H_r \\ F_i &= \mu_0 \varepsilon_{ijr} J_j H_r, \quad (i, j, r = (1 = x, 2 = y, 3 = z)) \end{aligned} \right\} \quad (1)$$

where $u_j = (u_x, u_y, u_z)$ refers to the tensor of displacement, $u_{j,t}$ is the particle velocity, and μ_0 stands for magnetic permeability. The symbols $\sigma_0 = n_e t_\xi e^2 / m_e$ denote the electrical conductivity of semiconductor material at the time of electronic deformation, e stands for electron charge, n_e stands for electron number density, t_ξ represents the electron’s collision time, m_e is the electron mass, ε_{ijr} stands for permutation, and F_i stands for the Lorentz force that gauges the force pressure of a magnetic field. Assuming that the strong, extremely magnetic field H_0 falls on the medium’s outer surface, the induced electric field is assumed to vanish, or $E = 0$. For a 1D deformation in the x -axis direction, we may express the displacement amount as $u_i = (u_x(x, t), 0, 0) = (u, 0, 0)$; the strain tensor is $e = u_x = \frac{\partial u}{\partial x}$. Ohm’s law of conduction (Equation (1)), on the other hand, expresses the current density components as: $J_1 = J_x = 0$, and $J_2 = J_y = 0$, but the z -axis can be written as [25]:

$$J_3 = J_z = \frac{\sigma_0 \mu_0 H_0}{1 + m^2} \left(\frac{\partial u}{\partial t} \right) \quad (2)$$

To get the Hall current parameter $m = t_\xi \omega_e$, we solve Equation (2), where $\omega_e = e \mu_0 H_0 / m_e$ is the electron frequency. For a 1D electronic/thermoelastic deformation, however, the magnetic field strength may be calculated using Lorentz’s force $F_i = (F_x, 0, 0)$, which can be rewritten as follows [25,26]:

$$F_x = \left(\frac{\sigma_0 \mu_0^2 H_0^2}{1 + m^2} \right) \frac{\partial u}{\partial t} \quad (3)$$

Free holes and electrons in a diffusive semiconductor material follow a steady stream or plasma distribution. Yet, unbound electrons and holes somewhat alter their course after colliding with internal particles. The free electrons and holes within a semiconductor are pushed in a 1D direction when a laser or light beam and an external magnetic field are applied to the material. When this occurs at photo-excited energies, or when holes and electrons interact, the other three 1D quantities may be included for analysis. The carrier density is $N(x, t)$, which reduces the electron charge carrier’s efficiency and masseurs the concentration of electrons (plasma wave). The thermal influence of the medium or thermal waves is measured by the temperature, $T(x, t)$. However, $H(x, t)$, which measures the hole charge carrier, can be used to describe the concentration of holes. The principal equations that describe the link between thermal, photo-electronic, elastic, and hole fields under the effect of magnetic fields and laser pulses with a power intensity of the laser p according to the coefficient of optical absorption δ in 1D can be expressed in the absence of body forces as [13]:

$$\left. \begin{aligned} &K(1 + \tau_\theta \frac{\partial}{\partial t}) \frac{\partial^2 T}{\partial x^2} + m_{nq} \frac{\partial^2 N}{\partial x^2} + m_{hq} \frac{\partial^2 H}{\partial x^2} - \rho(a_1^n \frac{\partial N}{\partial t} + a_1^h \frac{\partial H}{\partial t}) - \\ &(1 + \tau_q \frac{\partial}{\partial t}) \left[\rho C_e \frac{\partial T}{\partial t} + \rho T_0 \alpha_n \frac{\partial N}{\partial t} + \rho T_0 \alpha_h \frac{\partial H}{\partial t} + T_0 \gamma \frac{\partial}{\partial x} \frac{\partial u}{\partial t} \right] - \\ &\left[\frac{\rho a_1^n}{t^n} N + \frac{\rho a_1^h}{t^h} H \right] = (1 + \tau_q \frac{\partial}{\partial t}) p \delta e^{-(\Omega t + \delta x)} \end{aligned} \right\} \quad (4)$$

$$\left. \begin{aligned} &m_{qn} \frac{\partial^2 T}{\partial x^2} + D_n \rho \frac{\partial^2 N}{\partial x^2} - \rho(1 - a_2^n T_0 \alpha_n + t^n \frac{\partial}{\partial t}) \frac{\partial N}{\partial t} \\ &- a_2^n \left[\rho C_e \frac{\partial T}{\partial t} + \rho T_0 \alpha_n \frac{\partial H}{\partial t} + T_0 \gamma \frac{\partial}{\partial x} \frac{\partial u}{\partial t} \right] + \frac{\rho}{t^n} (1 + t^n \frac{\partial}{\partial t}) N = 0 \end{aligned} \right\} \quad (5)$$

$$\left. \begin{aligned} &m_{qh} \frac{\partial^2 T}{\partial x^2} + D_h \rho \frac{\partial^2 H}{\partial x^2} - \rho(1 - a_2^h T_0 \alpha_h + t^h \frac{\partial}{\partial t}) \frac{\partial H}{\partial t} \\ &- a_2^h \left[\rho C_e \frac{\partial T}{\partial t} + \rho T_0 \alpha_n \frac{\partial N}{\partial t} + T_0 \gamma \frac{\partial}{\partial x} \frac{\partial u}{\partial t} \right] + \frac{\rho}{t^h} (1 + t^h \frac{\partial}{\partial t}) H = 0 \end{aligned} \right\} \quad (6)$$

where the pulse parameter is Ω . The Hall current phenomenon, which illustrates the effects of electrical current flowing through a semiconductor media subjected to a strong magnetic field, might be used to formulate the corresponding equation of motion [12,25]:

$$\rho \frac{\partial^2 u}{\partial t^2} = (2\mu + \lambda) \frac{\partial^2 u}{\partial x^2} - \gamma(1 + \tau_\theta \frac{\partial}{\partial t}) \frac{\partial T}{\partial x} - \delta_n \frac{\partial N}{\partial x} - \delta_h \frac{\partial H}{\partial x} - \left(\frac{\sigma_0 \mu_0^2 H_0^2}{1 + m^2} \right) \frac{\partial u}{\partial t} \tag{7}$$

Equation (7) is differentiated with respect to x , and the result is:

$$\rho \frac{\partial^2 e}{\partial t^2} = (2\mu + \lambda) \frac{\partial^2 e}{\partial x^2} - \gamma(1 + \tau_\theta \frac{\partial}{\partial t}) \frac{\partial^2 T}{\partial x^2} - \delta_n \frac{\partial^2 N}{\partial x^2} - \delta_h \frac{\partial^2 H}{\partial x^2} - \left(\frac{\sigma_0 \mu_0^2 H_0^2}{1 + m^2} \right) \frac{\partial e}{\partial t} \tag{8}$$

where $a_1^n = \frac{a_{Qn}}{a_Q}$, $a_1^h = \frac{a_{Qh}}{a_Q}$, $a_2^n = \frac{a_{Qn}}{a_n}$ and $a_2^h = \frac{a_{Qh}}{a_h}$.

In terms of the associated thermal, photo-electric, elastic, and hole fields, the constitutive relation (stress) for 1D deformation may be expressed as follows:

$$\sigma_{xx} = \sigma = -(\gamma(1 + \tau_\theta \frac{\partial}{\partial t})T + \delta_n N + \delta_h H) + (2\mu + \lambda)e \tag{9}$$

Here is a considerable reduction of the dimensionless quantities:

$$\left. \begin{aligned} x', u' &= \frac{\omega^*(x,u)}{C_T}, (t', \tau_q', \tau_\theta', t^{n'}, t^{h'}, t_1^{n'}, t_1^{h'}) = \omega^*(t, \tau_q, \tau_\theta, t^n, t^h, t_1^n, t_1^h), C_L^2 = \frac{\mu}{\rho}, \\ \beta^2 &= \frac{C_T^2}{C_L^2}, k = \frac{K}{\rho C_e}, \sigma'_{ij} = \frac{\sigma_{ij}}{2\mu + \lambda}, N' = \frac{\delta_n(N)}{2\mu + \lambda}, C_T^2 = \frac{2\mu + \lambda}{\rho}, \Omega' = \frac{\Omega K}{\rho C_e C_T^2}, \\ \delta' &= \frac{\delta K}{\rho C_e C_T}, \omega^* = \frac{C_e(\lambda + 2\mu)}{K}, (\bar{\delta}_n, \bar{\delta}_h) = \left(\frac{\delta_n n_0, \delta_h h_0}{\gamma T_0} \right), T' = \frac{\gamma(T)}{2\mu + \lambda}, H' = \frac{\delta_h(H)}{2\mu + \lambda} \end{aligned} \right\} \tag{10}$$

For the sake of convenience, removing the primes from Equations (4)–(6), (8) and (9) results in:

$$\left\{ \begin{aligned} &\left(1 + \tau_\theta \frac{\partial}{\partial t}\right) \frac{\partial^2}{\partial x^2} - \left(1 + \tau_q \frac{\partial}{\partial t}\right) \frac{\partial}{\partial t} \Big\} T + \left\{ \alpha_1 \frac{\partial^2}{\partial x^2} - \alpha_2 \left(1 + \tau_q \frac{\partial}{\partial t}\right) - \alpha_3 \frac{\partial}{\partial t} - \alpha_4 \right\} N + \\ &\left\{ \alpha_5 \frac{\partial^2}{\partial x^2} - \left(1 + \tau_\alpha \frac{\partial}{\partial t}\right) \alpha_6 - \alpha_7 \right\} H - \left(1 + \tau_q \frac{\partial}{\partial t}\right) \varepsilon_1 \frac{\partial e}{\partial t} = \left(1 + \tau_q \frac{\partial}{\partial t}\right) \Gamma_1 e^{-(\Omega t + \delta x)} \end{aligned} \right\} \tag{11}$$

$$\left\{ \begin{aligned} &\left\{ \frac{\partial^2}{\partial x^2} - \alpha_8 \frac{\partial}{\partial t} \right\} T + \left\{ \alpha_9 \frac{\partial^2}{\partial x^2} - (\alpha_{10} + t^n \frac{\partial}{\partial t}) \alpha_{11} + (1 + t^n \frac{\partial}{\partial t}) \frac{\alpha_{11}}{t^n} \right\} N - \\ &\alpha_{12} \frac{\partial H}{\partial t} - \alpha_{13} \frac{\partial e}{\partial t} = 0 \end{aligned} \right\} \tag{12}$$

$$\left\{ \begin{aligned} &\left\{ \frac{\partial^2}{\partial x^2} - \alpha_{18} \frac{\partial}{\partial t} \right\} T + \left\{ \alpha_{14} \frac{\partial^2}{\partial x^2} - (\alpha_{15} + t^h \frac{\partial}{\partial t}) \alpha_{16} \frac{\partial}{\partial t} + (1 + t^h \frac{\partial}{\partial t}) \alpha_{17} \right\} H - \\ &\alpha_{19} \frac{\partial N}{\partial t} - \alpha_{20} \frac{\partial e}{\partial t} = 0 \end{aligned} \right\} \tag{13}$$

$$\left[\frac{\partial^2}{\partial x^2} - \frac{\partial^2}{\partial t^2} - \frac{M}{1 + m^2} \frac{\partial}{\partial t} \right] e - (1 + \tau_\theta \frac{\partial}{\partial t}) \frac{\partial^2 T}{\partial x^2} - \frac{\partial^2 N}{\partial x^2} - \alpha_{21} \frac{\partial^2 H}{\partial x^2} = 0 \tag{14}$$

$$e - H - (N + (1 + \tau_\theta \frac{\partial}{\partial t})T) = \sigma \tag{15}$$

$M = \frac{\sigma_0 t^* \mu_0^2 H_0^2}{\rho}$ denotes the number of magnetic pressure, or Hartmann number, that is present. However, the coefficients in the aforementioned equations are:

$$\begin{aligned} \alpha_1 &= \frac{m_{mq} \alpha_t}{d_n K}, \alpha_2 = \frac{T_0 \alpha_n}{C_e}, \alpha_3 = \frac{a_1^n}{C_e}, \alpha_4 = \frac{a_1^n \gamma}{C_e \tau^n (2\mu + \lambda)}, \alpha_5 = \frac{\gamma m_{hq} h_0}{(2\mu + \lambda) K}, \alpha_6 = \frac{T_0 \alpha_h K h_0}{C_e}, \\ \alpha_7 &= \frac{a_1^h \gamma \omega^*}{t^h K}, \alpha_8 = \frac{a_2^n K}{m_{qn}}, \alpha_9 = \frac{D_n \rho \alpha_t}{m_{qn} d_n}, \alpha_{10} = 1 - a_2^n T_0 \alpha_n, \alpha_{11} = \frac{\alpha_t K}{m_{qn} d_n C_e}, \alpha_{12} = \frac{a_2^n \gamma h_0 \alpha_h \omega^*}{m_{qn}}, \\ \alpha_{13} &= \frac{a_2^n \gamma^2 T_0 \omega^*}{\rho m_{gn}}, \alpha_{14} = \frac{D_n h_0 \gamma}{C_1^2 m_{qh}}, \alpha_{15} = 1 - a_2^h T_0 \alpha_n, \alpha_{16} = \frac{\gamma h_0 \omega^*}{m_{qh}}, \alpha_{17} = \frac{\gamma h_0 \omega^*}{m_{qh} \tau_1^h}, \alpha_{18} = a_2^h \frac{K}{m_{qh}}, \\ \alpha_{19} &= \frac{a_2^h \gamma T_0 \alpha_n (2\mu + \lambda) \omega^*}{m_{qh} \delta_n}, \alpha_{20} = \frac{a_2^h \gamma^2 T_0 \omega^*}{m_{qh} \rho}, \alpha_{21} = \frac{\delta_h}{\rho (2\mu + \lambda)}, \Gamma_1 = \frac{p \delta (1 - \tau_q \Omega)}{\rho C_e C_T}, \varepsilon_1 = \frac{T_0 \gamma^2 \omega^*}{\rho K}, \end{aligned}$$

which indicates the thermoelastic coupling parameters ε_1 and α_1 to α_{21} displays the optical-elastic-thermal coupling parameters.

To approach the issue theoretically, a few initial conditions are introduced. The initial conditions in this scenario can be thought of with the homogeneity qualities as follows:

$$\begin{aligned} e(x, t)|_{t=0} &= \frac{\partial e(x, t)}{\partial t} \Big|_{t=0} = 0, \quad T(x, t)|_{t=0} = \frac{\partial T(x, t)}{\partial t} \Big|_{t=0} = 0, \\ H(x, t)|_{t=0} &= \frac{\partial H(x, t)}{\partial t} \Big|_{t=0} = 0, \quad N(x, t)|_{t=0} = \frac{\partial N(x, t)}{\partial t} \Big|_{t=0} = 0 \end{aligned} \tag{16}$$

3. The Mathematical Analysis

The engineering problem can be studied using Laplace transforms, which can be built for function $\Sigma(x, t)$ as:

$$L(\Sigma(x, t)) = \bar{\Sigma}(x, s) = \int_0^\infty \exp(-st) \Sigma(x, t) dt \tag{17}$$

Laplace transformations on the dimensionless fundamental system (11)–(16) with the assistance of the initial conditions Equation (16) produce:

$$(q_1 D^2 - q_2) \bar{T} + (\alpha_1 D^2 - q_3) \bar{N} + (\alpha_5 D^2 - q_4) \bar{H} - q_5 \bar{e} = \Gamma_2 e^{-\delta x} \tag{18}$$

$$(D^2 - q_7) \bar{T} + (\alpha_9 D^2 - q_6) \bar{N} - q_8 \bar{H} - q_9 \bar{e} = 0 \tag{19}$$

$$(D^2 - q_{10}) \bar{T} + (\alpha_{14} D^2 - q_{11}) \bar{H} - q_{12} \bar{N} - q_{13} \bar{e} = 0 \tag{20}$$

$$(D^2 - \Re_H) \bar{e} - q_{14} D^2 \bar{T} - D^2 \bar{N} - \alpha_{21}^* D^2 \bar{H} = 0 \tag{21}$$

$$\bar{\sigma}_{xx} = \alpha_{23} (\bar{e} - ((1 + s\tau_\theta) \bar{T} + \bar{N})) - \bar{H} \tag{22}$$

where $q_1 = (1 + \tau_\theta \frac{\partial}{\partial t})$, $\Re_H = s^2 + s \frac{M}{1+m^2}$, $q_2 = (1 + \tau_q \frac{\partial}{\partial t}) s$, $\Gamma_2 = \frac{\Gamma_1 (1 + \tau_q s)}{s + \Omega}$, $q_4 = (1 + \tau_q \frac{\partial}{\partial t}) \alpha_6 + \alpha_7$, $q_3 = (\alpha_2 (1 + \tau_q \frac{\partial}{\partial t}) + \alpha_3 \frac{\partial}{\partial t} + \alpha_4)$, $q_6 = (\alpha_{10} + t^n s) \alpha_{11} - (1 + t^n s) \frac{\alpha_{11}}{t^n}$, $\alpha_{21}^* = \frac{\delta_h}{(2\mu + \lambda)}$, $D = \frac{d}{dx}$, $q_5 = (1 + \tau_q s) \varepsilon_1 s$, $q_7 = \alpha_8 s$, $q_8 = \alpha_{12} s$, $q_{12} = \alpha_{19} s$, $q_{13} = \alpha_{20} s$, $q_{14} = 1 + \tau_\theta s$, $q_9 = \alpha_{13} s$, $q_{10} = \alpha_{18} s$, $q_{11} = (\alpha_{15} + t^h s) \alpha_{16} s - (1 + t^h s) \alpha_{17}$.

Major-quantity \bar{T} , \bar{u} , \bar{N} and \bar{H} solutions may be found using the elimination technique of the system of Equations (17)–(20). In this situation, the equation that follows can be written as:

$$(D^8 - \Pi_1 D^6 + \Pi_2 D^4 - \Pi_3 D^2 + \Pi_4) \{ \bar{H}, \bar{T}, \bar{e}, \bar{N} \} (x, s) = \Xi e^{-\delta x} \tag{23}$$

where $\Xi = \frac{\Gamma_1(\delta^2 q_2 - s^2)}{(s + \Omega)}$. On the other hand, the main coefficients of Equation (23), which have the following form, can be determined using computer programming software (Mathematica):

$$\Pi_1 = \frac{-1}{(\alpha_9 \alpha_{14} q_1 - \alpha_1 \alpha_{14} - \alpha_5 \alpha_9)} \left(\alpha_{14} q_1 (\Re_H \alpha_9 - \alpha_1 q_{14}) + \alpha_9 q_{14} (\alpha_5 q_{13} + \alpha_{14} q_5) + \alpha_{21}^* \alpha_9 q_{13} q_1 - \alpha_1 \alpha_{14} (\Re_H + q_7) - \alpha_1 \alpha_{21}^* q_9 - \alpha_9 q_4 - \alpha_1 \alpha_{21}^* q_{13} - \alpha_5 \alpha_9 q_{10} + \alpha_{14} \alpha_9 q_2 - \alpha_9 \alpha_{21}^* q_5 + \alpha_9 q_1 q_{11} + \alpha_{14} q_1 q_6 + q_6 (\alpha_{14} q_1 - \alpha_5) - \alpha_1 (q_{11} - q_8) + \alpha_5 (q_{12} + q_{13}) - \alpha_{14} (q_3 + q_5) \right) \quad (24)$$

$$\Pi_2 = \frac{1}{(\alpha_9 \alpha_{14} q_1 - \alpha_1 \alpha_{14} - \alpha_5 \alpha_9)} \left(\Re_H (\alpha_9 \alpha_{14} q_1 + \alpha_9 (\alpha_5 q_{10} - \alpha_{14} q_2 - q_1 q_{11}) - \alpha_{14} q_1 q_6) + \alpha_1 (\alpha_{21} q_7 q_{13} - \alpha_{21}^* q_9 q_{10} - q_{14} (q_8 q_{13} - q_9 q_{11})) + \alpha_5 q_{14} (q_6 q_{13} - q_9 q_{12}) - \alpha_9 \alpha_{21}^* (q_2 q_{13} - q_5 q_{10}) + \alpha_9 q_{14} (q_4 q_{13} - q_5 q_{11}) + \alpha_{14} q_{14} (q_3 q_9 - q_5 q_6) - \alpha_{21}^* q_1 (q_6 q_{13} + q_9 q_{12}) - \Re_H (\alpha_1 (q_8 - q_{11}) + \alpha_5 q_{12} - \alpha_9 q_4 - \alpha_{14} q_3) + \alpha_1 (q_7 q_{11} - q_8 q_{10}) + \alpha_5 (q_6 q_{10} - q_7 (q_{12} + q_{13}) + q_9 q_{10}) - \alpha_9 (q_2 q_{11} - q_4 q_{10}) - \alpha_{14} (q_2 (q_6 - q_9) - \alpha_{21}^* (q_3 q_{13} - q_5 (q_6 + q_{12})) - q_7 (q_3 + q_7) - q_1 (q_6 q_{11} - q_8 (q_{12} + q_{13}) + q_9 q_{11}) - q_5 (q_8 - q_{11}) - q_3 (q_8 - q_{11}) + q_4 (q_6 + q_9 - q_{12} + q_{13})) \right) \quad (25)$$

$$\Pi_4 = \frac{\Re_H (-q_2 q_6 q_{11} + q_2 q_8 q_{12} + q_3 (q_7 q_{11} - q_8 q_{10}) + q_4 (q_6 q_{10} - q_7 q_{12}))}{(-\alpha_9 \alpha_{14} q_1 + \alpha_1 \alpha_{14} + \alpha_5 \alpha_9)} \quad (26)$$

$$\Pi_3 = \frac{-1}{(\alpha_9 \alpha_{14} q_1 - \alpha_1 \alpha_{14} - \alpha_5 \alpha_9)} \left\{ \Re_H (\alpha_1 q_8 q_{10} - \alpha_1 q_7 q_{11} - \alpha_5 q_6 q_{10} + \alpha_5 q_7 q_{12} + \alpha_9 (q_2 q_{11} - q_4 q_{10}) + \alpha_{14} (q_2 q_6 - q_3 q_7) + q_1 (q_6 q_{11} - q_8 q_{12})) + \alpha_{21}^* (q_2 (q_6 q_{13} - q_9 q_{12}) - q_3 (q_7 q_{13} - q_9 q_{10}) - q_5 (q_6 q_{10} - q_7 q_{12})) + q_3 q_{14} (q_8 q_{13} - q_9 q_{11}) - q_4 q_{14} (q_6 q_{13} - q_9 q_{12}) - q_5 q_{14} (q_6 q_{11} - q_8 q_{12}) + \Re_H (q_3 (q_8 - q_{11}) - q_4 (q_6 - q_{12})) + q_2 (q_6 q_{11} - q_8 q_{12} - q_8 q_{13} + q_9 q_{11}) - q_3 (q_7 q_{11} - q_8 q_{10}) - q_4 (q_6 q_{10} - q_7 (q_{12} + q_{13}) + q_9 q_{10}) + q_5 (q_8 q_{10} - q_8 q_{10}) \right\} \quad (27)$$

The correct roots of Equation (23) may be found by factoring as follows:

$$(D^2 - m_1^2) (D^2 - m_2^2) (D^2 - m_3^2) (D^2 - m_4^2) \{ \bar{T}, \bar{e}, \bar{N}, \bar{H} \} (x, s) = \Xi e^{-\delta x} \quad (28)$$

where $m_i^2 (i = 1, 2, 3, 4)$ stands for the roots of the auxiliary equation, which are found when $x \rightarrow \infty$. In this case, we may choose any one of the four positive real components of the roots. For the main field, linearity yields a rewrite of the answers as:

$$\bar{T}(x, s) = \sum_{i=1}^4 B_i(s) e^{-m_i x} + \mathbb{Q} e^{-\delta x} \quad (29)$$

Nonetheless, linear solutions exist for the following physical values:

$$\bar{N}(x, s) = \sum_{i=1}^4 B'_i(s) e^{-m_i x} + f_1(s) e^{-\delta x} = \sum_{i=1}^4 H_{1i} B_i(s) e^{-m_i x} + f_1(s) e^{-\delta x} \quad (30)$$

$$\bar{e}(x, s) = \sum_{i=1}^4 B''_i(s) e^{-m_i x} + f_2(s) e^{-\delta x} = \sum_{i=1}^4 H_{2i} B_i(s) e^{-m_i x} + f_2(s) e^{-\delta x} \quad (31)$$

$$\bar{H}(x, s) = \sum_{i=1}^4 B'''_i(s) e^{-m_i x} + f_3(s) e^{-\delta x} = \sum_{i=1}^4 H_{3i} B_i(s) e^{-m_i x} + f_3(s) e^{-\delta x} \quad (32)$$

$$\bar{\sigma}(x, s) = \sum_{i=1}^4 (B''''_i(s)) e^{-m_i x} + f_4(s) e^{-\delta x} = \sum_{i=1}^4 (H_{4i} B_i(s)) e^{-m_i x} + f_4(s) e^{-\delta x} \quad (33)$$

where

$$\begin{aligned} \mathbb{Q} &= \Xi(\delta^8 - \Pi_1 \delta^6 + \Pi_2 \delta^4 - \Pi_3 \delta^2 + \Pi_4) \\ H_{1i} &= -\frac{\alpha_{14}m_i^6 + c_7m_i^4 + c_8m_i^2 + c_9}{\alpha_9\alpha_{14}m_i^6 + c_4m_i^4 + c_5m_i^2 + c_6}, \\ H_{2i} &= \frac{c_{10}m_i^6 + c_{11}m_i^4 + c_{12}m_i^2}{\alpha_9\alpha_{14}m_i^6 + c_4m_i^4 + c_5m_i^2 + c_6}, \\ H_{3i} &= -\frac{\alpha_9m_i^6 + c_1m_i^4 + c_2m_i^2 + c_3}{\alpha_9\alpha_{14}m_i^6 + c_4m_i^4 + c_5m_i^2 + c_6}, \\ H_{4i} &= \alpha_{23}(H_{2i} - ((1 + s\tau_\theta)H_{1i} + 1) - \alpha_{22}H_{3i}), \\ c_1 &= -(q_6 + q_9 - q_{12} - q_{13}) + \alpha_9(-q_{13}q_{14} - R_H - q_{10}), \\ c_2 &= R_H\alpha_9q_{10} + q_9q_{13}q_{14} - q_9q_{12}q_{14} + R_H(q_6 - q_{12}) + q_6q_{10} - q_7q_{12} - q_7q_{13} + q_9q_{10}, \\ c_3 &= R_H(q_7q_{12} - q_6q_{10}), \\ c_4 &= -R_H(\alpha_9\alpha_{14} - \alpha_9\alpha_{21}q_{13} - \alpha_9q_{11} - \alpha_{14}q_6 - \alpha_{14}q_9), \\ c_5 &= R_H\alpha_9q_{11} + R_H\alpha_{14}q_6 + \alpha_{21}q_6q_{13} - \alpha_{21}q_9q_{12} + q_6q_{11} - q_8q_{12} - q_8q_{13} + q_9q_{11}, \\ c_6 &= R_H(q_8q_{12} - q_6q_{11}), \\ c_7 &= \alpha_{14}(-q_9q_{14} - R_H - q_7) + \alpha_{21}(q_9 - q_{13}) + q_8 - q_{11}, \\ c_8 &= R_H\alpha_{14}q_7 + \alpha_{21}(q_7q_{13} - q_9q_{10}) - q_8q_{13}q_{14} + q_9q_{11}q_{14} - R_H(q_8 - q_{11}) + q_7q_{11} - q_8q_{10}, \\ c_9 &= R_H(-q_7q_{11} + q_8q_{10}), \\ c_{10} &= \alpha_9(\alpha_{14}q_{14} - \alpha_{21} - \alpha_{14}), \\ c_{11} &= \alpha_9\alpha_{21}q_{10} + \alpha_9q_{11}q_{14} - \alpha_{14}q_6q_{14} - q_8q_{12}q_{14} + \alpha_{14}q_7 + \alpha_{21}(q_6 - q_{12}) - q_8 + q_{11}, \\ c_{12} &= -\alpha_{21}q_6q_{10} + \alpha_{21}q_7q_{12} + q_6q_{11}q_{14} - q_8q_{12}q_{14} - q_7q_{11} + q_8q_{10}, \\ f_1 &= \mathbb{Q} \frac{c_1\delta^4 + c_2\delta^2 + c_3}{c_4\delta^4 + c_5\delta^2 + c_6}, \\ f_2 &= -\mathbb{Q} \left\{ \frac{-(\delta^2q_1 - q_2)q_9\delta - q_5\delta(\delta - q_7)}{-(\delta^2\alpha_5 - q_4)q_9\delta + q_5q_8\delta} - \frac{(-(\delta\alpha_1 - q_3)q_9\delta - q_5\delta(\delta^2\alpha_9 - q_6))H_{3i}}{-(\delta^2\alpha_5 - q_4)q_9\delta + q_5q_8\delta} \right\}, \\ f_3 &= \mathbb{Q} \left\{ \frac{(\delta^2q_1 - q_2)}{q_5\delta} + \frac{(\delta^2\alpha_5 - q_4)H_{2i}}{q_5\delta} + \frac{(\delta^2\alpha_1 - q_3)H_{1i}}{q_5\delta} \right\}, \\ f_4 &= \mathbb{Q}(\alpha_{23}(\delta H_{2i} - ((1 + s\tau_\theta)H_{1i} + 1) - \alpha_{22}H_{3i})). \end{aligned}$$

4. Boundary Conditions

The parameters' values may be determined by subjecting the semiconductor's free surface to a controlled set of environmental conditions, as there are no limits to the medium at infinity.

(I) The Laplace transform was obtained at the free surface ($x = 0$) after being treated to an exponential heat flux of pulse (Figure 2). The pulsing heat flow boundary condition may be shown in the following ways using the thermal gradient temperature:

$$\left. \frac{\partial T(x, t)}{\partial x} \right|_{x=0} = -q_0 \frac{t^2 e^{-\frac{t}{t_p}}}{16t_p^2} \quad (34)$$

where t_p represents the pulse heat flux time and q_0 is an arbitrary constant. When the Laplace transform is applied to the thermal condition (I), together with the dimensionless property, we get:

$$\left. \frac{\partial T(r, s)}{\partial x} \right|_{x=0} = -\frac{q_0 t_p}{8(1 + pt_p)^3} \quad (35)$$

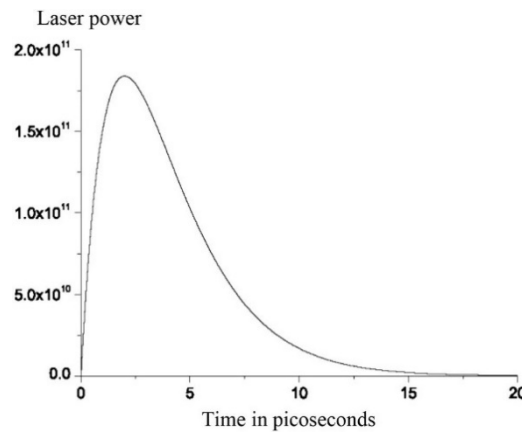


Figure 2. Temporal profile of the laser pulse.

(II) For the normal stress component at $x = 0$, the mechanical ramp type can be applied as:

$$\sigma(x, t) = \begin{cases} 0 & t \leq 0 \\ \frac{t}{t_0} & 0 < t \leq t_0 \\ 1 & t > t_0 \end{cases} \quad (36)$$

Nevertheless, using Equation (33), we obtain:

$$\sum_{i=1}^4 H_{4i} B_i(s) + f_4(s) = \bar{F}(s) \frac{(1 - e^{-st_0})}{t_0 s^2} \quad (37)$$

(III) During one-dimensional ablation with a pulsed heating source, the physical and thermal models between photoionization and photothermal ionization are investigated. Surface recombination activities in the setting of photo-excitation with diffusion might potentially choose the plasma state. The carrier density is transformed when using the Laplace method:

$$\bar{N}(0, s) = \frac{\tilde{s}\lambda n_0}{D_e} \quad (38)$$

Equation (30), which results in:

$$\sum_{i=1}^4 H_{1i} B_i(s) + f_1(s) = \frac{\lambda \tilde{s} n_0}{D_e} \quad (39)$$

(IV) In addition, the surface of the recombination diffusion with photo-excitation processes exhibits a hole charge carrier field, which can be selected in the equilibrium situation as (at $x = 0$):

$$\bar{H}(0, s) + f_3(s) = h_0 \quad (40)$$

Equation (32) results in:

$$\sum_{i=1}^4 H_{3i} B_i(s) = h_0 \quad (41)$$

in the relationships mentioned above. \tilde{s} stands for recombination speed, D_e is the electron charge diffusion coefficient, and λ stands for any arbitrary parameter. The parameters are found by algebraically resolving the preceding system of four Equations: (35), (37), (39) and (41).

5. Inversion of the Laplace Transform

The Laplace domain solutions have so far been found. The Laplace transform must be inverted to obtain solutions in the time domain. Yet, this cannot be conducted analytically

because of how complex the solution formulations are. Hence, the rapid Fourier transform-based numerical inversion of the Laplace transform (NILT) approach is implemented [40]. Laplace transform’s integral form provides an expression for the inverse of any function $\mathbb{Z}(x, s)$ under certain conditions:

$$\mathbb{Z}(x, t') = L^{-1}\{\overline{\mathbb{Z}}(x, s)\} = \frac{1}{2\pi i} \int_{n-i\infty}^{n+i\infty} \overline{\mathbb{Z}}(x, s) \exp(st') ds \tag{42}$$

In the time domain, we may rewrite Equation (42) as follows, which is the inversion approach:

$$\mathbb{Z}(x, t') = \frac{\exp(nt')}{2\pi} \int_{-\infty}^{\infty} \overline{\mathbb{Z}}(x, n + i\beta) \exp(i\beta t') d\beta \tag{43}$$

In the interval $[0, 2t']$, using Equation (43) as a guide, we may extend the function $\mathbb{Z}(x, t')$ into a closed form, yielding the following [37]:

$$\mathbb{Z}(x, t') = \frac{e^{nt'}}{t'} \left[Re \sum_{k=1}^M \overline{\mathbb{Z}}(x, n + \frac{ik\pi}{t'}) (-1)^k + \frac{1}{2} \overline{\mathbb{Z}}(x, n) \right] \tag{44}$$

where $i = \sqrt{-1}$, $n \in R$ (real numbers), M is freely selected, with the real part expressed by the symbol Re , and the approximate value is indicated by the notation $nt' \approx 4.7$.

6. Validation

6.1. The Photo-Thermoelasticity Models

In photo-thermoelasticity theory, there are three possible models that may be constructed using different values for the thermal and elastic relaxation times. The first phase-lag is represented by the parameter τ_θ , and the second phase-lag is represented by the value τ_q . Three models, however, can be found in this investigation:

- (1) $0 \leq \tau_\theta < \tau_q$; this yields the dual phase lag (DPL) model.
- (2) $\tau_\theta = 0, 0 < \tau_q$; this yields the Lord and Shulman (LS) model.
- (3) $\tau_\theta = \tau_q = 0.0$; this yields the coupled thermoelasticity (CT) model.

6.2. Effect of Magnetic Field

When $H_0 = 0$, the problem is examined without consideration for the effects of the Hall current, and the impact of a strong magnetic field is disregarded. However, when $H_0 \neq 0$, the effect of the magnetic field on the Hall current has been noticed and is taken into account.

6.3. Without Electron-Hole Interaction, Thermoelasticity Theory

When the impact of holes and electrons are discarded and just the magnetic field’s impact is considered, i.e., when $H = 0$ and $N = 0$, the issue may be investigated using the generalized thermoelasticity theory. Using simply the Hall current effect, the system of governing equations in this case is reduced to two equations under the effect of laser intensity as follows:

$$K(1 + \tau_\theta \frac{\partial}{\partial t}) \frac{\partial^2 T}{\partial x^2} - (1 + \tau_q \frac{\partial}{\partial t}) \left[\rho C_e \frac{\partial T}{\partial t} + T_0 \gamma \frac{\partial e}{\partial t} \right] = (1 + \tau_q \frac{\partial}{\partial t}) p \delta e^{-(\Omega t + \delta x)} \tag{45}$$

$$\rho \frac{\partial^2 e}{\partial t^2} = (2\mu + \lambda) \frac{\partial^2 e}{\partial x^2} - \gamma(1 + \tau_\theta \frac{\partial}{\partial t}) \frac{\partial^2 T}{\partial x^2} - \left(\frac{\sigma_0 \mu_0^2 H_0^2}{1 + m^2} \right) \frac{\partial e}{\partial t} \tag{46}$$

6.4. The Magneto-Photo-Thermoelasticity Theory

Since the influence of the holes field is ignored ($H = 0$), the issue can only be studied using the generalized magneto-photo-thermoelasticity theory. The magnetic field simplifies this example’s system of equations down to a simpler set of three equations:

$$m_{qn} \frac{\partial^2 T}{\partial x^2} + D_n \rho \frac{\partial^2 N}{\partial x^2} - \rho(1 - a_2^n T_0 \alpha_n + t^n \frac{\partial}{\partial t}) \frac{\partial N}{\partial t} - a_2^n \left[\rho C_e \frac{\partial T}{\partial t} + T_0 \gamma \frac{\partial e}{\partial t} \right] = \left. \begin{matrix} \\ - \frac{\rho}{t^n} (1 + t^n \frac{\partial}{\partial t}) N \end{matrix} \right\} \quad (47)$$

$$K(1 + \tau_\theta \frac{\partial}{\partial t}) \frac{\partial^2 T}{\partial x^2} - (1 + \tau_q \frac{\partial}{\partial t}) \left[\rho C_e \frac{\partial T}{\partial t} + \rho T_0 \alpha_n \frac{\partial N}{\partial t} + T_0 \gamma \frac{\partial e}{\partial t} \right] + \left. \begin{matrix} \\ m_{nq} \frac{\partial^2 N}{\partial x^2} - \rho a_1^n \frac{\partial N}{\partial t} = (1 + \tau_q \frac{\partial}{\partial t}) \rho \delta e^{-(\Omega t + \delta x)} \end{matrix} \right\} \quad (48)$$

$$\rho \frac{\partial^2 e}{\partial t^2} = (2\mu + \lambda) \frac{\partial^2 e}{\partial x^2} - \gamma(1 + \tau_\theta \frac{\partial}{\partial t}) \frac{\partial^2 T}{\partial x^2} - \delta_n \frac{\partial^2 N}{\partial x^2} - \delta_h \frac{\partial^2 H}{\partial x^2} - \left(\frac{\sigma_0 \mu_0^2 H_0^2}{1 + m^2} \right) \frac{\partial e}{\partial t} \quad (49)$$

6.5. The Non-Gaussian Laser Pulses Impact

The impact of non-Gaussian laser pulses is reflected in the fundamental equations that were discussed before. When the power intensity of the effect of the laser pulses is ignored (that is to say, when $p = 0$ is used), however, the model that is being studied transforms into a model of the generalized photo-thermoelasticity theory under the influence of electron and hole interactions only. In this case, Equation (4) can be rewritten in the form:

$$\left. \begin{matrix} K(1 + \tau_\theta \frac{\partial}{\partial t}) \frac{\partial^2 T}{\partial x^2} + m_{nq} \frac{\partial^2 N}{\partial x^2} + m_{hq} \frac{\partial^2 H}{\partial x^2} - \rho(a_1^n \frac{\partial N}{\partial t} + a_1^h \frac{\partial H}{\partial t}) - \\ (1 + \tau_q \frac{\partial}{\partial t}) \left[\rho C_e \frac{\partial T}{\partial t} + \rho T_0 \alpha_n \frac{\partial N}{\partial t} + \rho T_0 \alpha_h \frac{\partial H}{\partial t} + T_0 \gamma \frac{\partial}{\partial x} \frac{\partial u}{\partial t} \right] - \left[\frac{\rho a_1^n}{t^n} N + \frac{\rho a_1^h}{t^h} H \right] = 0 \end{matrix} \right\} \quad (50)$$

7. Numerical Results and Discussions

Temperature, strain, carrier density, hole carrier charge field, and stress may all be computed and graphically represented in 1D in the time domain using the Riemann sum approximation and numerical inversion of the Laplace transform. Silicon (Si) is a semiconductor material that might be used in this hypothetical situation. Here, Table 1 displays the input parameters (in SI units) used for the Si material and the magnetic field parameters (from [37–39]):

Table 1. The physical parameters in SI units for Si materials.

Unit	Symbol	Value
N/m ²	λ	6.4×10^{10}
	μ	6.5×10^{10}
kg/m ³	ρ	2330
K	T_0	800
sec (s)	τ	5×10^{-5}
K ⁻¹	α_t	4.14×10^{-6}
Wm ⁻¹ K ⁻¹	k	150
J/(kg K)	C_e	695
m/s	\tilde{s}	2
H/m	μ_0	$4\pi \times 10^{-7}$

Table 1. *Cont.*

Unit	Symbol	Value
vk ⁻¹	m_{qn}	1.4×10^{-5}
	m_{nq}	1.4×10^{-5}
	m_{qh}	-0.004×10^{-6}
	m_{hq}	-0.004×10^{-6}
m ² s ⁻¹	D_n	0.35×10^{-2}
m ² s ⁻¹	D_h	0.125×10^{-2}
m ² /s	α_n	1×10^{-2}
m ² /s	α_h	5×10^{-3}

7.1. The Photo-Electronic-Thermoelasticity Models

The first group of images in Figure 3 illustrates the instantaneous axial distributions of the primary real dimensional fields (small time $t = 0.0004$). It is possible to create models of photo-thermoelasticity exposed to a strong magnetic field and the Hall current effect by comparing how much thermal relaxation times vary when the influence of laser pulses is incorporated. The thermal wave under the impact of the laser heat flux condition applied at the outer surface of the silicon medium is shown in the first inset for examination of the dimensionless temperature distributions. The effects of optical-thermal excitation, laser pulses, and magnetic field pressure are depicted in the first subfigure, showing that the dimensionless thermal wave values begin as positive, increase to a maximum value near the medium's edge, and then decrease as distance increases until they approach the zero line, satisfying the stability state. In contrast, the growth of the thermal wave was exponential. The second panel shows the distribution of normal stress (mechanical waves) throughout the axial distance. The mechanical wave distributions exhibit the requisite abrupt increase from a positive value at the edge to a peak-maximum value towards the surface that is characteristic of mechanical ramps (due to the pressure force of a strong magnetic field or Hall current and laser pulse effect). The mechanical wave weakens as it moves away from the surface, and this weakening continues until the wave approaches the zero line, where it seeks equilibrium. The third inset depicts the impact of thermal and elastic relaxation time on the dimensional hole carrier charge distribution throughout the axial distance (thermal memory). The hole carrier charge distributions start with positive maximum values at the boundary edge and quickly decline to the lowest peak after recombination with the plasma. However, in the second region, the hole carrier charge distributions once again grow, stabilize locally within the material for a brief period of time, and then fall to the stable state through convergence to the zero line. Plasma recombination processes cause the carrier density, which represents plasma waves (the dispersion of the electron charge field), to start off with a positive value at the edge, as seen in the fourth inset. Plasma waves, driven by optical-thermal energy and a Hall current, peak abruptly at the surface, then retreat gradually according to an exponential decay curve as they travel into the semiconductor medium. When the plasma waves approach the zero line, stability is achieved. According to experimental observations, the distribution decreases exponentially with distance from the surface until it reaches equilibrium at the zero line inside the semiconductor medium [41,42].

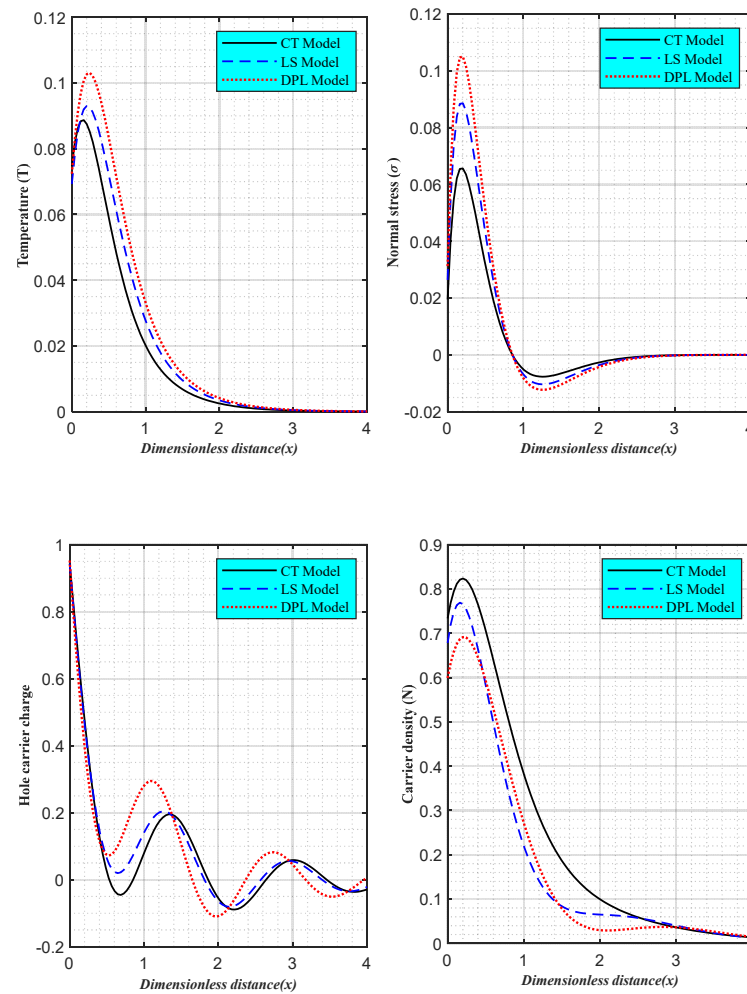


Figure 3. Under the influence of the Hall current and laser pulses, the principal physical distributions vary with distance in accordance with photo-electronic-thermoelasticity theories.

7.2. The Impact of Hall's Current

The second set of equations illustrates the effect of laser pulses on the fundamental field distributions T , σ , H , and N as a function of axial distance x in a magnetic field subject to Hall current influence (Figure 4). In this study, we examine two scenarios in which the DPL model is applied to silicon semiconductor material for a low-time operation. When the Hall current is present and the Hartmann number (the strength of magnetic pressure) is not zero, as seen in the first image, the fundamental field distribution changes. The second example shows how physical fields are distributed when there is no strong magnetic field or Hall current. Particles inside the semiconductor medium clash forcefully due to optical stimulation and the compressive intensity of the strong magnetic field created by the Hall current (plasma) and laser pulses. All physical values exhibit a wave-like behavior in the absence of magnetic stimulation, which is distinct from the current condition. However, when a strong magnetic field is paired with a Hall current, the semiconductor lattice's interior particles are rearranged (along with the spindle movement of particles). By raising the concentration of holes and free electrons on the semiconductor's surface, the Hall current boosts the flow of electric current within the material.

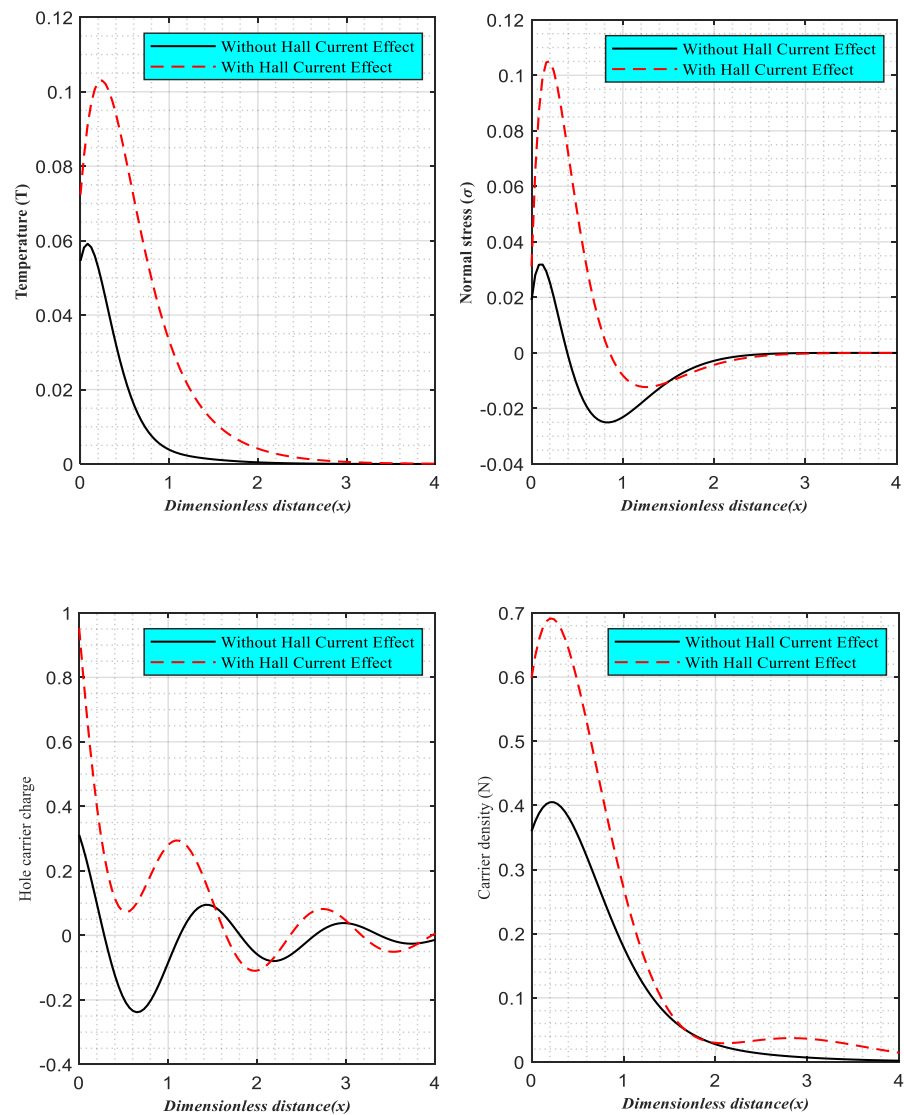


Figure 4. Hall current's influence on the distribution of main fields with distance, as predicted by the DPL model, when exposed to laser pulses.

7.3. The Laser Pulses Effect

The third group shows the effect of a laser pulse, plotting the major field distributions versus the laser's power intensity (Figure 5). This study looks at two scenarios by applying the DPL model to Hall's current effects on silicon semiconductor materials over short periods. The presence of laser intensity is shown in the first subfigure, which depicts the distribution of basic fields. In the second subfigure, physical fields are shown to be distributed when no laser pulses are present. Optical stimulation, laser pulses, and the compressive intensity of a strong magnetic field in conjunction with the Hall current cause internal particles in the semiconductor medium to smash violently, resulting in a cloud of surface electrons (plasma). In this situation, all physical values propagate differently as waves compared to when there is no laser impact. Yet, in the presence of laser pulses, the semiconductor lattice undergoes a reorganization of its interior particles (through spindle movement of particles). By increasing the number of holes and free electrons on the semiconductor's surface, the laser pulse increases the flow of electric current within the semiconductor.

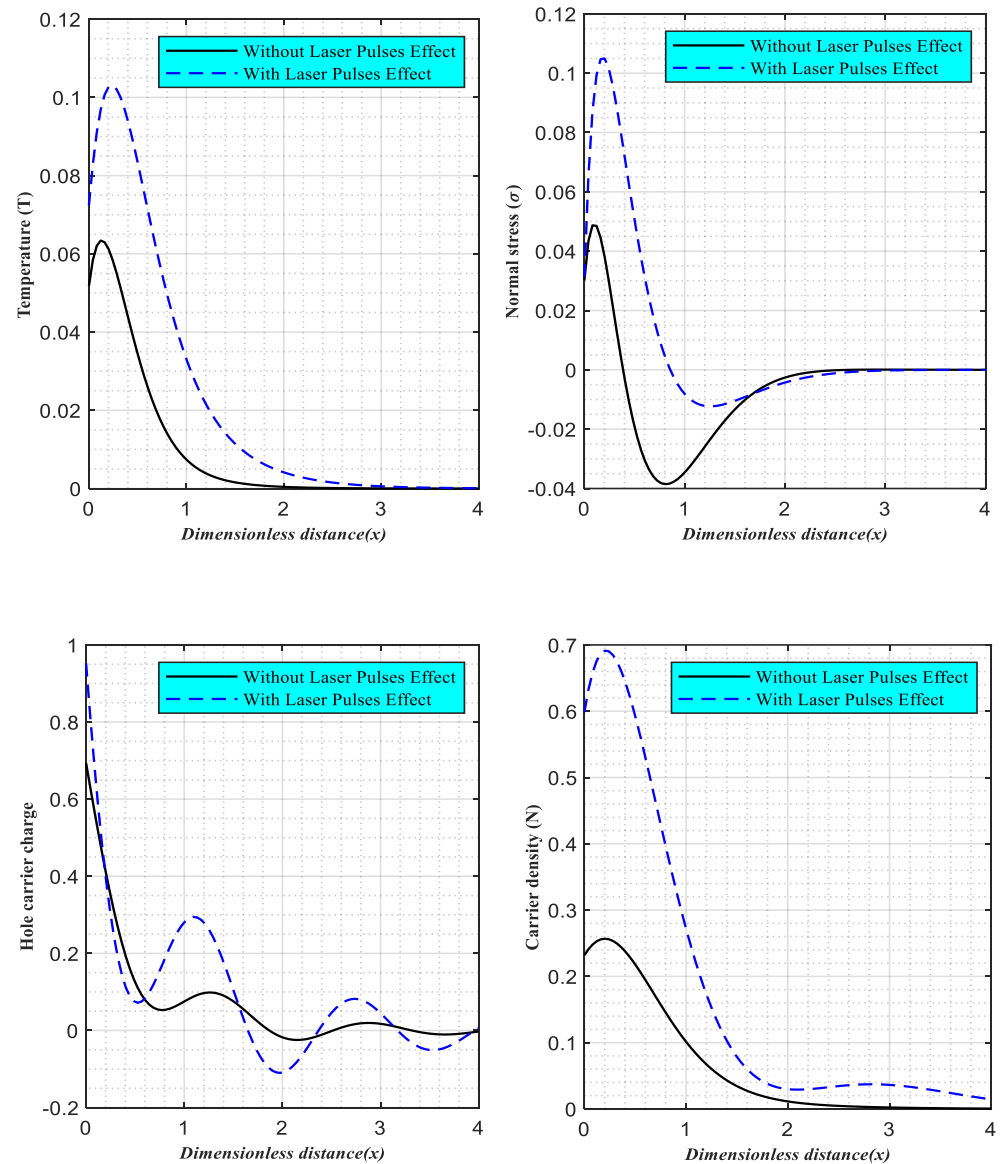


Figure 5. The dependence on distance of the principal field distributions induced by laser pulses in the DPL model with Hall current is analyzed.

7.4. The 3D Graph

As anticipated by the DPL model for Si media, Figure 6 (the fourth group) shows three-dimensional (3D) graphs affected by laser pulses and a high magnetic field through the Hall current effect. This diagram looks at how time and distance affect the wave distribution of basic physical properties when the dimensionless period $0 \leq t \leq 4 \times 10^{-2}$ may be obtained. In this class, the propagation of waves is affected by the passage of time in all physical domains, satisfying the boundary conditions. The magnitude of wave propagations, however, varies across all physical domains as a function of axial distance and time scale variances. According to the steady state, all wave propagation vanishes and approaches the zero line when increasing the distance and time.

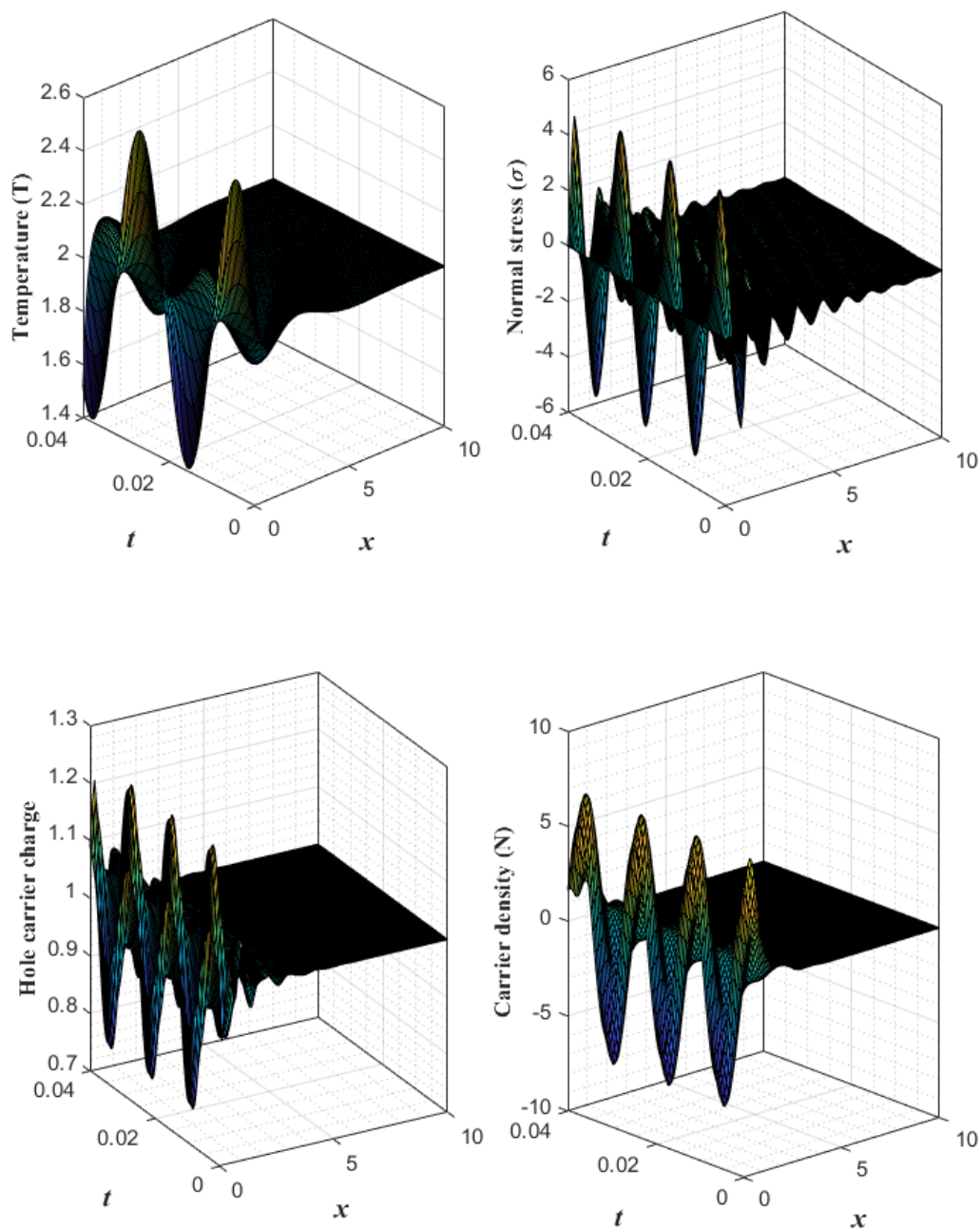


Figure 6. The effect of laser pulses and Hall current on the spatial and temporal distributions of the principal fields in three dimensions, as predicted by the DPL model.

8. Conclusions

This study looked at how a strong magnetic field affects the movement of photo-thermoelastic waves induced by laser pulses in a semiconducting material. Hole and electron interactions during 1D elastic and electronic deformation have inspired a novel model. Photo-excited diffusion and the role of optical energy were considered. The pressure force of a strong magnetic field causes the Hall current with a Hartmann number to be generated. Very few literature reviews have examined the impact of a laser pulse and the Hall current effect on the interaction between holes and electrons. The difference between the relaxation time and the time value affects the wave propagation of the physical distributions in every case. The Hall current, a byproduct of the powerful magnetic field, also affects the wave propagation of the physical quantities of interest. Waves of the physical variables under study are modified by the laser pulses. This is because certain

materials, especially semiconductors, may experience changes in response to the magnetic field and laser pulse, as predicted by scientific theory. As a result, the Hall current provides researchers with a wealth of information about semiconductors, linear Hall sensors, and Hall potentiometers. The Hall effects have widespread applications in many fields of science and technology, such as those dealing with automation, measurement, and electronics.

Author Contributions: N.B.: methodology, software; K.L.: validation, formal analysis; N.G.: investigation, resources; K.L.: data curation; A.A.E.-B.: writing—review and editing; visualization K.L.: supervision. All authors have read and agreed to the published version of the manuscript.

Funding: Deanship of Scientific Research at Northern Border University, the grant No. ENGA-2022-11-1938, Northern Border University, Arar, K.S.A.

Data Availability Statement: The datasets used and/or analyzed during the current study are available from the corresponding author on reasonable request.

Acknowledgments: The authors gratefully acknowledge the approval and the support of this research study under the grant No. ENGA-2022-11-1938 from the Deanship of Scientific Research at Northern Border University, Arar, K.S.A.

Conflicts of Interest: The authors declare no conflict of interest.

Nomenclature

λ, μ	Lame's constants,
n_0	Electrons concentration
h_0	Holes concentration
T_0	Absolute temperature
$\gamma = (3\lambda + 2\mu)\alpha_t$	The volume coefficient of thermal expansion
σ_{ij}	Stress tensor
ρ	Density
α_n, α_h	Thermo-diffusive parameters of Electrons and Holes
τ_q, τ_θ	The thermal and elastic relaxation times
t^h, t^n	The holes and electron's relaxation times
α_t	The linear thermal expansion coefficient
C_e	Specific heat
K	Thermal conductivity
τ^*	The photo-generated carrier lifetime
E_g	The energy gap
$\delta_n = (2\mu + 3\lambda)d_n$	The electron's elasto-diffusive parameter
$\delta_h = (2\mu + 3\lambda)d_h$	The holes elasto-diffusive parameter
d_n	The coefficients of electronic deformation
d_h	The coefficient of holes deformation
$m_{nq}, m_{qn}, m_{hq}, m_{qh}$	Peltier-Dufour- Seebeck-Soret-like constants
D_n, D_h	The diffusion coefficient of the electrons and holes
$a_{Qn}, a_{Qh}, a_Q, a_n, a_h$	The flux-like constants

References

- Hall, E. On a New Action of the Magnet on Electric Currents. *Am. J. Math.* **1879**, *2*, 287–292. [[CrossRef](#)]
- Klitzing, K.; Dorda, G.; Pepper, M. New Method for High-Accuracy Determination of the Fine-Structure Constant Based on Quantized Hall Resistance. *Phys. Rev. Lett.* **1980**, *45*, 494–497. [[CrossRef](#)]
- Mendez, E.; Esaki, L.; Chang, L. Quantum Hall Effect in a Two-Dimensional Electron-Hole Gas. *Phys. Rev. Lett.* **1985**, *55*, 2216–2219. [[CrossRef](#)] [[PubMed](#)]
- Büttiker, M. Absence of backscattering in the quantum Hall effect in multiprobe conductors. *Phys. Rev. B* **1988**, *38*, 9375–9389. [[CrossRef](#)]
- Takashina, K.; Nicholas, R.J.; Kardynal, B.; Mason, N.J.; Maude, D.K.; Portal, J.C. Breakdown of the quantum Hall effect in an electron-hole system. *Phys. B Condens. Matter* **2001**, *298*, 8–12. [[CrossRef](#)]
- Biot, M.A. Thermoelasticity and irreversible thermodynamics. *J. Appl. Phys.* **1956**, *27*, 240–253. [[CrossRef](#)]
- Lord, H.; Shulman, Y. A generalized dynamical theory of Thermoelasticity. *J. Mech. Phys. Solids* **1967**, *15*, 299–309. [[CrossRef](#)]

8. Green, A.E.; Lindsay, K.A. Thermoelasticity. *J. Elast.* **1972**, *2*, 1–7. [[CrossRef](#)]
9. Chandrasekharaiah, D.S. Thermoelasticity with second sound: A review. *Appl. Mech. Rev.* **1986**, *39*, 355–376. [[CrossRef](#)]
10. Chandrasekharaiah, D.S. Hyperbolic Thermoelasticity: A review of recent literature. *Appl. Mech. Rev.* **1998**, *51*, 705–729. [[CrossRef](#)]
11. Sharma, J.N.; Kumar, V.; Dayal, C. Reflection of generalized thermoelastic waves from the boundary of a half-space. *J. Therm. Stress.* **2003**, *26*, 925–942. [[CrossRef](#)]
12. Lotfy, K.; Abo-Dahab, S. Two-dimensional problem of two temperature generalized thermoelasticity with normal mode analysis under thermal shock problem. *J. Comput. Theor. Nanosci.* **2015**, *12*, 1709–1719. [[CrossRef](#)]
13. Othman, M.; Lotfy, K. The influence of gravity on 2-D problem of two temperature generalized thermoelastic medium with thermal relaxation. *J. Comput. Theor. Nanosci.* **2015**, *12*, 2587–2600. [[CrossRef](#)]
14. Maruszewski, B. Electro-magneto-thermo-elasticity of Extrinsic Semiconductors, Classical Irreversible Thermodynamic Approach. *Arch. Mech.* **1986**, *38*, 71–82.
15. Maruszewski, B. Electro-magneto-thermo-elasticity of Extrinsic Semiconductors, Extended Irreversible Thermodynamic Approach. *Arch. Mech.* **1986**, *38*, 83–95.
16. Maruszewski, B. Coupled Evolution Equations of Deformable Semiconductors. *Int. J. Eng. Sci.* **1987**, *25*, 145–153. [[CrossRef](#)]
17. Sharma, J.; Thakur, N. Plane harmonic elasto-thermodiffusive waves in semiconductor materials. *J. Mech. Mater. Struct.* **2006**, *1*, 813–835. [[CrossRef](#)]
18. Mandelis, A. *Photoacoustic and Thermal Wave Phenomena in Semiconductors*; Elsevier: Alharetta, GA, USA, 1987.
19. Almond, D.; Patel, P. *Photothermal Science and Techniques*; Springer Science & Business Media: Berlin, Germany, 1996.
20. Gordon, J.P.; Leite, R.C.C.; Moore, R.S.; Porto, S.P.S.; Whinnery, J.R. Long-transient effects in lasers with inserted liquid samples. *Bull. Am. Phys. Soc.* **1964**, *119*, 501. [[CrossRef](#)]
21. Lotfy, K. Effect of variable thermal conductivity during the photothermal diffusion process of semiconductor medium. *Silicon* **2019**, *11*, 1863–1873. [[CrossRef](#)]
22. Lotfy, K.; Tantawi, R.S. Photo-thermal-elastic interaction in a functionally graded material (FGM) and magnetic field. *Silicon* **2020**, *12*, 295–303. [[CrossRef](#)]
23. Lotfy, K. A novel model of magneto photothermal diffusion (MPD) on polymer nano-composite semiconductor with initial stress. *Waves Ran. Comp. Med.* **2021**, *31*, 83–100. [[CrossRef](#)]
24. Lotfy, K.; El-Bary, A.; Hassan, W.; Ahmed, M. Hall current influence of microtemperature magneto-elastic semiconductor material. *Superlattices Microstruct.* **2020**, *139*, 106428. [[CrossRef](#)]
25. Mahdy, A.; Lotfy, K.; Ahmed, M.; El-Bary, A.; Ismail, E. Electromagnetic Hall current effect and fractional heat order for microtemperature photo-excited semiconductor medium with laser pulses. *Results Phys.* **2020**, *17*, 103161. [[CrossRef](#)]
26. Mahdy, A.; Lotfy, K.; El-Bary, A.; Tayel, I. Variable thermal conductivity and hyperbolic two-temperature theory during magneto-photothermal theory of semiconductor induced by laser pulses. *Eur. Phys. J. Plus* **2021**, *136*, 651. [[CrossRef](#)]
27. Lotfy, K. The elastic wave motions for a photothermal medium of a dual-phase-lag model with an internal heat source and gravitational field. *Can. J. Phys.* **2016**, *94*, 400–409. [[CrossRef](#)]
28. Lotfy, K. A Novel Model of Photothermal Diffusion (PTD) fo Polymer Nano- composite Semiconducting of Thin Circular Plate. *Phys. B Condens. Matter* **2018**, *537*, 320–328. [[CrossRef](#)]
29. Lotfy, K.; Kumar, R.; Hassan, W.; Gabr, M. Thermomagnetic effect with microtemperature in a semiconducting Photothermal excitation medium. *Appl. Math. Mech. Engl. Ed.* **2018**, *39*, 783–796. [[CrossRef](#)]
30. Mahdy, A.; Lotfy, K.; El-Bary, A.; Sarhan, H. Effect of rotation and magnetic field on a numerical-refined heat conduction in a semiconductor medium during photo-excitation processes. *Eur. Phys. J. Plus* **2021**, *136*, 553. [[CrossRef](#)]
31. Lotfy, K. A novel model for Photothermal excitation of variable thermal conductivity semiconductor elastic medium subjected to mechanical ramp type with two-temperature theory and magnetic field. *Sci. Rep.* **2019**, *9*, 3319. [[CrossRef](#)]
32. Marin, M. On existence and uniqueness in thermoelasticity of micropolar bodies. *Comptes Rendus Acad. Sci. Ser. II Fasc. B* **1995**, *321*, 375–480.
33. Marin, M.; Marinescu, C. Thermoelasticity of initially stressed bodies, Asymptotic equipartition of energies. *Int. J. Eng. Sci.* **1998**, *36*, 73–86. [[CrossRef](#)]
34. Alzahrani, F.; Hobiny, A.; Abbas, I.; Marin, M. An eigenvalues approach for a two-dimensional porous medium based upon weak, normal and strong thermal conductivities. *Symmetry* **2020**, *12*, 848. [[CrossRef](#)]
35. Scutaru, M.; Vlase, S.; Marin, M.; Modrea, A. New analytical method based on dynamic response of planar mechanical elastic systems. *Bound. Value Probl.* **2020**, *2020*, 104. [[CrossRef](#)]
36. Marin, M.; Ellahi, R.; Vlase, S.; Bhatti, M. On the decay of exponential type for the solutions in a dipolar elastic body. *J. Taibah Univ. Sci.* **2020**, *14*, 534–540. [[CrossRef](#)]
37. Singh, A.; Das, S.; Altenbach, H.; Craciun, E.-M. Semi-infinite moving crack in an orthotropic strip sandwiched between two identical half planes. *ZAMM Z. Angew. Math. Mech.* **2020**, *100*, e201900202. [[CrossRef](#)]
38. Mondal, S.; Sur, A. Photo-thermo-elastic wave propagation in anorthotropic semiconductor with a spherical cavity and memory responses. *Waves Random Complex Media* **2021**, *31*, 1835–1858. [[CrossRef](#)]
39. Abbas, I.; Alzahrani, F.; Elaiwb, A. A DPL model of photothermal interaction in a semiconductor material. *Waves Random Complex Media* **2019**, *29*, 328–343. [[CrossRef](#)]

40. Brancik, L. Programs for fast numerical inversion of Laplace transforms in MATLAB language environment. In Proceedings of the 7th Conference MATLAB, Prague, Czech Republic; 1999; Volume 99, pp. 27–39.
41. Xiao, Y.; Shen, C.; Zhang, W. Screening and prediction of metal-doped α -borophene monolayer for nitric oxide elimination. *Mater. Today Chem.* **2022**, *25*, 100958. [[CrossRef](#)]
42. Liu, J.; Han, M.; Wang, R.; Xu, S.; Wang, X. Photothermal phenomenon: Extended ideas for thermophysical properties characterization. *J. Appl. Phys.* **2022**, *131*, 065107. [[CrossRef](#)]

Disclaimer/Publisher's Note: The statements, opinions and data contained in all publications are solely those of the individual author(s) and contributor(s) and not of MDPI and/or the editor(s). MDPI and/or the editor(s) disclaim responsibility for any injury to people or property resulting from any ideas, methods, instructions or products referred to in the content.